

Available online at [www.sciencedirect.com](http://www.sciencedirect.com)

journal homepage: [www.elsevier.com/locate/ajps](http://www.elsevier.com/locate/ajps)

## Original Research Paper

# Glycosylated and non-glycosylated quantum dot-displayed peptides trafficked indiscriminately inside lung cancer cells but discriminately sorted in normal lung cells: An indispensable part in nanoparticle-based intracellular drug delivery

Roger Salvacion Tan <sup>a,b,\*</sup><sup>a</sup> Department of Chemistry, College of Science, De La Salle University, 2401 Taft Avenue, Manila 0922 Philippines<sup>b</sup> Department of Chemistry, College of Science and Mathematics, Mindanao State University-Iligan Institute of Technology, A. Bonifacio Avenue, Tibanga, Iligan City 9200 Philippines

## ARTICLE INFO

## Article history:

Received 25 May 2017

Received in revised form 17 August 2017

Accepted 4 December 2017

Available online 8 December 2017

## Keywords:

Intracellular trafficking  
 Peptides and glycopeptides  
 Lung cancer cells  
 Normal lung tissue  
 Golgi localization  
 Quantum dots

## ABSTRACT

Difference in sub-cellular trafficking of glycosylated and naked peptides, between normal and lung cancer cells, was established. Normal lung tissue discriminately sorted glycosylated from non-glycosylated peptides by allowing golgi localization of the glycosylated peptides while restricting golgi entry of the naked peptides. This mechanism was surprisingly not observed in its cancer cell counterpart. Lung cancer cells tend to allow unrestricted localization of both glycosylated and naked peptides in the golgi apparatus. This newly discovered difference in sub-cellular trafficking between normal and lung cancer cells could potentially be used as an effective strategy in targeted intracellular delivery, especially targeting golgi-resident enzymes for possible treatment of diseases associated with glycans and glycoproteins, such as, congenital disease of glycosylation (CDG). This very important detail in intracellular trafficking inside normal and cancer cells is an indispensable part in nanoparticle-based intracellular drug delivery.

© 2018 Shenyang Pharmaceutical University. Production and hosting by Elsevier B.V. This is an open access article under the CC BY-NC-ND license (<http://creativecommons.org/licenses/by-nc-nd/4.0/>).

\* Department of Chemistry, De La Salle University, 2401 Taft Avenue, Manila 0922, Philippines. Tel.: +63 2 5360230.

E-mail address: [roger.tan@dlsu.edu.ph](mailto:roger.tan@dlsu.edu.ph).

Peer review under responsibility of Shenyang Pharmaceutical University.

<https://doi.org/10.1016/j.ajps.2017.12.002>1818-0876/© 2018 Shenyang Pharmaceutical University. Production and hosting by Elsevier B.V. This is an open access article under the CC BY-NC-ND license (<http://creativecommons.org/licenses/by-nc-nd/4.0/>).

## 1. Introduction

Protein glycosylation is one of the most common post-translational modifications employed by biological systems to expand proteome diversity [1-3]. Glycosylation is evolutionarily found to occur in proteins through the main domains of life [4,5] and has been shown to influence a variety of critical biological processes such as protein folding, protein stability, trafficking, localization, and protein-protein binding, with important implications for cell-cell interactions, intracellular signaling, and intracellular targeting [6,7]. The specific conformational changes in protein, either exogenously incorporated or endogenously expressed in cells, as a consequence of protein glycosylation [8-12] could alter the overall structure of protein and potentially alter their functions, intracellular route, and recognition mechanism. Therefore, it is not surprising that a substantial fraction of the approved protein pharmaceuticals need to be properly glycosylated to exhibit optimal therapeutic efficacy [13,14].

Glycans associated with cell surface receptors and proteins do not only alter the dynamics of glycoprotein endocytosis but also their cell surface half-life through binding to multi-valent lectins [15]. Glycan structures on newly synthesized proteins are crucial for protein secretion, as they influence protein folding, provide ligands for lectin chaperones, contribute to quality control surveillance in the endoplasmic reticulum (ER) and mediate transit, trafficking, and selective protein targeting throughout the secretory pathways [16,17]. Hence, in the presence of glycans, protein or peptide could potentially be trafficked inside the cell differently.

Biological and therapeutic molecules are also trafficked to distinct cellular compartments through both biosynthetic and endocytic pathways. Delivering pharmacological agents to cells via these endocytic pathways require knowledge and understanding of the trafficking itinerary and the molecular dynamics of the organelles concerned [18-22]. These pathways are vital to pave the way in understanding intracellular drug delivery and to give insights into the real-time dynamics of exogenous molecules, including nanoparticle-based delivery of therapeutic agents, as they are delivered into and traffic within single cell [23,24].

Despite emerging importance of quantum dot (QD)-based delivery of peptides [25,26] and glycans [27-29], which are promising tools both in general cell biology and discovery research for diagnostic/therapeutic agents, there are no direct, systematic, and substantial studies on the direct evidence of intracellular sorting/trafficking mechanisms of peptides and glycopeptides, as well as the differences in their intracellular incorporation on both normal and cancer cell lines. There is no other concrete way to compare the effect of the presence and absence of glycosylation, in terms of intracellular trafficking and compartmentalization, than comparing its behavior inside normal and cancer cells of same types.

In this study, difference in intracellular localization and trafficking of peptides and glycopeptides in both normal and lung cancer cell lines were investigated. QD-based delivery of peptides and glycopeptides were performed to observe the difference in intracellular localization mechanism.

## 2. Materials and methods

### 2.1. Materials

All Fmoc-protected amino acids and PyBOP were purchased from Novabiochem, HBTU was from Peptide Institute Inc. HOBt was from Kokusan Kagaku Corp. HOAt was from GenScript. Rink-amide-ChemMatrix resin was from Biotage. N-(9-Fluorenylmethoxycarbonyl)-O-[2,3-di-O-acetyl-4-O-(2,3,4,6-tetra-O-acetyl- $\beta$ -D-galactopyranosyl)- $\beta$ -D-xylopyranosyl]-L-Serine was purchased from Medicinal Chemistry Pharmaceutical Ltd., Japan (<http://soyaku.co.jp/>). Coating reagents, 11,11'-dithio bis[undec-11-yl 12-(aminooxyacetyl)amino hexa(ethyleneglycol)] (AOSH) and a phosphoryl derivative, 11-mercaptoundecylphosphorylcholine (PCSH) were synthesized by the procedures reported previously and available from MCP Co. Ltd. Qdot 545 ITK™, Lysotracker Red DND-99, and Hoechst 33342 were from Invitrogen. DCM, DMF, DIEA and TFA were purchased from Watanabe Chem. IND., LTD. Ultrafiltration membranes were supplied from Millipore, Carrigtwohill, Co. Cork, Ireland. Unless otherwise noted, solvents and other reagents were purchased from Aldrich Chemical Co. (Milwaukee, WI), Tokyo Chemical Industry (Tokyo, Japan), and Wako Pure Chemical Industries Ltd. (Tokyo, Japan).

### 2.2. Synthesis of peptides and glycopeptides

#### 2.2.1. Synthesis of ketone-functionalized compound 1

A 0.24 mmol/g of Rink-amide-ChemMatrix resin, Fmoc-Ser(tBu)-OH (96  $\mu$ mol, 4.0 equivalents), Fmoc-Gly-OH (96  $\mu$ mol, 4.0 equivalents) and 5-oxohexanoic acid (4.0 equivalents) were used. Briefly, 0.24 mmol/g of Rink-amide-ChemMatrix resin was placed in a 5 ml Libra tube, washed sequentially with DMF and DCM followed by DCM swelling for 30 min. The swollen resin was washed with DMF. Fmoc-amino acid was pre-activated using 4 equivalents of HBTU, 4 equivalents of HOBt in DMF and 3 equivalents of DIEA for 30 sec. The pre-activated Fmoc-amino acid was then added to the resin and allowed to couple for 15 min at 50 °C under microwave irradiation. The resin was then washed subsequently with DMF, DCM and then DMF. To block the unreacted/uncoupled amino groups in the resin, acetyl capping was performed using DMF:Ac<sub>2</sub>O:DIEA (8.5:1.0:0.5) for 5 min at room temperature, washed with DMF, DCM and then DMF, then Fmoc deprotection using 20% piperidine in DMF followed by washing with DMF, DCM and then DMF and the cycle repeated for alternating Ser-Gly sequence. After Fmoc deprotection of the last Fmoc-amino acid, 5-oxohexanoic acid was pre-activated using 4 equivalents of HBTU, 4 equivalents of HOBt in DMF and 3 equivalents of DIEA for 30 sec. The pre-activated 5-oxohexanoic acid was then added to the peptide-resin mixture and allowed to couple for 15 min at 50 °C under microwave irradiation. The mixture was washed subsequently with DMF, DCM and then DMF. Deprotected and cleavage of the peptide from the resin was done by adding TFA:H<sub>2</sub>O (95: 5) cocktail to the washed resin in ice for 30 min with shaking and then the shaking was continued at room temperature for additional 1 h. The deprotection and cleavage processes were monitored using MALDI-TOF/MS. The solution containing the synthesized peptide was drained. The resin

was flushed subsequently with the same cocktail solution, acetic acid, and methanol. The filtrates were combined and concentrated by air drying, dissolved in 50% acetonitrile and lyophilized. The peptide was then purified using RP-HPLC with acetonitrile (B) and water (A) both with 0.1% TFA using Intersil® ODS-3 (5 µm, 4.6 mm x 250 mm) column at room temperature, 1 ml/min flow rate, 220 nm wavelength for detection, and solvent gradient (A:B) of 99:1 (0 min), 85:15 (50 min), and 5:95 (60 min) to get compound 1, then lyophilized [29–32].

MALDI-TOF/MS:  $m/z$  calcd for  $C_{16}H_{27}N_5NaO_8^+$ ,  $[M + Na]^+$  440.1757, found 440.195.

#### 2.2.2. Synthesis of ketone-functionalized compound 2

A 0.24 mmol/g of Rink-amide-ChemMatrix resin, Fmoc-Ser(tBu)-OH (96 µmol, 4.0 equivalents), Fmoc-Gly-OH (96 µmol, 4.0 equivalents), *N*-(9-Fluorenylmethoxycarbonyl)-*O*-[2,3-di-*O*-acetyl-4-*O*-(2,3,4,6-tetra-*O*-acetyl-β-*D*-galactopyranosyl)-β-*D*-xylopyranosyl]-*L*-Serine (MCP Co., Ltd, Japan) (36 µmol, 1.5 equivalents) and 5-oxohexanoic acid (4.0 equivalents) were used. Briefly, 0.24 mmol/g of Rink-amide-ChemMatrix resin was placed in a 5 ml Libra tube, washed sequentially with DMF and DCM followed by DCM swelling for 30 min. The swollen resin was washed with DMF. Fmoc-amino acid was pre-activated using 4 equivalents of HBTU, 4 equivalents of HOBT in DMF and 3 equivalents of DIEA for 30 sec. The pre-activated Fmoc-amino acid was then added to the resin and allowed to couple for 15 min at 50 °C under microwave irradiation. The resin was then washed subsequently with DMF, DCM and then DMF. To block the unreacted/uncoupled amino groups in the resin, acetyl capping was performed using DMF:Ac<sub>2</sub>O:DIEA (8.5:1.0:0.5) for 5 min at room temperature, washed with DMF, DCM and then DMF, then Fmoc deprotection using 20% piperidine in DMF followed by washing with DMF, DCM and then DMF and the cycle repeated for alternating Ser-Gly sequence. For the introduction of *N*-(9-Fluorenylmethoxycarbonyl)-*O*-[2,3-di-*O*-acetyl-4-*O*-(2,3,4,6-tetra-*O*-acetyl-β-*D*-galactopyranosyl)-β-*D*-xylopyranosyl]-*L*-Serine, 1.2 equivalents of PyBOP, 1.2 equivalents of HOAt in DMF and 3 equivalents of DIEA as the coupling cocktail. After coupling for 15 min at 50 °C under microwave irradiation, the same coupling cocktail, without Fmoc-glycoamino acid, was added for a “double activation-like” approach for 15 min at 50 °C under microwave irradiation. After Fmoc deprotection of the last Fmoc-amino acid, 5-oxohexanoic acid was pre-activated using 4 equivalents of HBTU, 4 equivalents of HOBT in DMF and 3 equivalents of DIEA for 30 sec. The pre-activated 5-oxohexanoic acid was then added to the peptide-resin mixture and allowed to couple for 15 min at 50 °C under microwave irradiation. The mixture was washed subsequently with DMF, DCM and then DMF. Deprotected and cleavage of the peptide from the resin was done by adding TFA:H<sub>2</sub>O (95: 5) cocktail to the washed resin in ice for 30 min with shaking and then the shaking was continued at room temperature for additional 1 h. The deprotection and cleavage processes were monitored using MALDI-TOF/MS. The solution containing the synthesized glycopeptide was drained. The resin was flushed subsequently with the same cocktail solution, acetic acid, and methanol. The filtrates were combined and concentrated by air drying, dissolved in 50% acetonitrile and lyophilized. The peptide was then purified using RP-HPLC with acetonitrile (B) and water (A) both with 0.1% TFA using Intersil® ODS-3 (5 µm,

4.6 mm x 250 mm) column at room temperature, 1 ml/min flow rate, 220 nm wavelength for detection, and then lyophilized. The purified glycopeptide was de-*O*-acetylated by dissolving in trifluoroethanol and added with sodium hydroxide to pH 10.5–11.0 for 30 min. The removal of the acetyl groups from the sugar moiety was monitored using MALDI-TOF/MS. After the complete deacetylation process, the solvent was removed either under reduced pressure or air-drying. The de-*O*-acetylated glycopeptide was purified by RP-HPLC with acetonitrile (B) and water (A) both with 0.1% TFA using Intersil® ODS-3 (5 µm, 4.6 mm x 250 mm) column at room temperature, 1 ml/min flow rate, 220 nm wavelength for detection, and solvent gradient (A:B) of 99:1 (0 min), 85:15 (50 min), and 5:95 (60 min) to get compound 2 and then lyophilized [29–32].

MALDI-TOF/MS:  $m/z$  calcd for  $C_{27}H_{45}N_5NaO_{17}^+$ ,  $[M + Na]^+$  734.2708, found 734.409.

#### 2.2.3. Synthesis of ketone-functionalized compound 3

A 0.24 mmol/g of Rink-amide-ChemMatrix resin, Fmoc-Ser(tBu)-OH (96 µmol, 4.0 equivalents), Fmoc-Gly-OH (96 µmol, 4.0 equivalents), and 5-oxohexanoic acid (4.0 equivalents) were used. Briefly, 0.24 mmol/g of Rink-amide-ChemMatrix resin was placed in a 5 ml Libra tube, washed sequentially with DMF and DCM followed by DCM swelling for 30 min. The swollen resin was washed with DMF. Fmoc-amino acid was pre-activated using 4 equivalents of HBTU, 4 equivalents of HOBT in DMF and 3 equivalents of DIEA for 30 sec. The pre-activated Fmoc-amino acid was then added to the resin and allowed to couple for 15 min at 50 °C under microwave irradiation. The resin was then washed subsequently with DMF, DCM and then DMF. To block the unreacted/uncoupled amino groups in the resin, acetyl capping was performed using DMF:Ac<sub>2</sub>O:DIEA (8.5:1.0:0.5) for 5 min at room temperature, washed with DMF, DCM and then DMF, then Fmoc deprotection using 20% piperidine in DMF followed by washing with DMF, DCM and then DMF and the cycle repeated for alternating Ser-Gly sequence. After Fmoc deprotection of the last Fmoc-amino acid, 5-oxohexanoic acid was pre-activated using 4 equivalents of HBTU, 4 equivalents of HOBT in DMF and 3 equivalents of DIEA for 30 sec. The pre-activated 5-oxohexanoic acid was then added to the peptide-resin mixture and allowed to couple for 15 min at 50 °C under microwave irradiation. The mixture was washed subsequently with DMF, DCM and then DMF. Deprotected and cleavage of the peptide from the resin was done by adding TFA:H<sub>2</sub>O (95: 5) cocktail to the washed resin in ice for 30 min with shaking and then the shaking was continued at room temperature for additional 1 h. The deprotection and cleavage processes were monitored using MALDI-TOF/MS. The solution containing the synthesized peptide was drained. The resin was flushed subsequently with the same cocktail solution, acetic acid, and methanol. The filtrates were combined and concentrated by air drying, dissolved in 50% acetonitrile and lyophilized. The peptide was then purified using RP-HPLC with acetonitrile (B) and water (A) both with 0.1% TFA using Intersil® ODS-3 (5 µm, 4.6 mm x 250 mm) column at room temperature, 1 ml/min flow rate, 220 nm wavelength for detection, and solvent gradient (A:B) of 99:1 (0 min), 85:15 (50 min), and 5:95 (60 min) to get compound 3 and then lyophilized [29–32].

MALDI-TOF/MS:  $m/z$  calcd for  $C_{66}H_{107}N_{25}NaO_{38}^+$ ,  $[M + Na]^+$  1880.7106, found 1880.082.

#### 2.2.4. Synthesis of ketone-functionalized compound 4

A 0.24 mmol/g of Rink-amide-ChemMatrix resin, Fmoc-Ser(tBu)-OH (96  $\mu$ mol, 4.0 equivalents), Fmoc-Gly-OH (96  $\mu$ mol, 4.0 equivalents), N-(9-Fluorenylmethoxycarbonyl)-O-[2,3-di-O-acetyl-4-O-(2,3,4,6-tetra-O-acetyl- $\beta$ -D-galactopyranosyl)- $\beta$ -D-xylopyranosyl]-L-Serine (MCP Co., Ltd, Japan) (36  $\mu$ mol, 1.5 equivalents) and 5-oxohexanoic acid (4.0 equivalents) were used. Briefly, 0.24 mmol/g of Rink-amide-ChemMatrix resin was placed in a 5 ml Libra tube, washed sequentially with DMF and DCM followed by DCM swelling for 30 min. The swollen resin was washed with DMF. Fmoc-amino acid was pre-activated using 4 equivalents of HBTU, 4 equivalents of HOBT in DMF and 3 equivalents of DIEA for 30 sec. The pre-activated Fmoc-amino acid was then added to the resin and allowed to couple for 15 min at 50 °C under microwave irradiation. The resin was then washed subsequently with DMF, DCM and then DMF. To block the unreacted/uncoupled amino groups in the resin, acetyl capping was performed using DMF:Ac<sub>2</sub>O:DIEA (8.5:1.0:0.5) for 5 min at room temperature, washed with DMF, DCM and then DMF, then Fmoc deprotection using 20% piperidine in DMF followed by washing with DMF, DCM and then DMF and the cycle repeated for alternating Ser-Gly sequence. For the introduction of N-(9-Fluorenylmethoxycarbonyl)-O-[2,3-di-O-acetyl-4-O-(2,3,4,6-tetra-O-acetyl- $\beta$ -D-galactopyranosyl)- $\beta$ -D-xylopyranosyl]-L-Serine, 1.2 equivalents of PyBOP, 1.2 equivalents of HOAt in DMF and 3 equivalents of DIEA as the coupling cocktail. After coupling for 15 min at 50 °C under microwave irradiation, the same coupling cocktail, without Fmoc-glycoamino acid, was added for a “double activation-like” approach for 15 min at 50 °C under microwave irradiation. After Fmoc deprotection of the last Fmoc-amino acid, 5-oxohexanoic acid was pre-activated using 4 equivalents of HBTU, 4 equivalents of HOBT in DMF and 3 equivalents of DIEA for 30 sec. The pre-activated 5-oxohexanoic acid was then added to the peptide-resin mixture and allowed to couple for 15 min at 50 °C under microwave irradiation. The mixture was washed subsequently with DMF, DCM and then DMF. Deprotected and cleavage of the peptide from the resin was done by adding TFA:H<sub>2</sub>O (95:5) cocktail to the washed resin in ice for 30 min with shaking and then the shaking was continued at room temperature for additional 1 h. The deprotection and cleavage processes were monitored using MALDI-TOF/MS. The solution containing the synthesized glycopeptide was drained. The resin was flushed subsequently with the same cocktail solution, acetic acid, and methanol. The filtrates were combined and concentrated by air drying, dissolved in 50% acetonitrile and lyophilized. The peptide was then purified using RP-HPLC with acetonitrile (B) and water (A) both with 0.1% TFA using Intersil® ODS-3 (5  $\mu$ m, 4.6 mm x 250 mm) column at room temperature, 1 ml/min flow rate, 220 nm wavelength for detection, and then lyophilized. The purified glycopeptide was de-O-acetylated by dissolving in trifluoroethanol and added with sodium hydroxide to pH 10.5–11.0 for 30 min. The removal of the acetyl groups from the sugar moiety was monitored using MALDI-TOF/MS. After the complete deacetylation process, the solvent was removed either under reduced pressure or air-drying. The de-O-acetylated glycopeptide was purified by RP-HPLC with acetonitrile (B) and water (A) both with 0.1% TFA using

Intersil® ODS-3 (5  $\mu$ m, 4.6 x 250 mm) column at room temperature, 1 ml/min flow rate, 220 nm wavelength for detection, and solvent gradient (A:B) of 99:1 (0 min), 85:15 (50 min), and 5:95 (60 min) to get compound 4 and then lyophilized [29–32].

MALDI-TOF/MS: *m/z* calcd for C<sub>132</sub>H<sub>215</sub>N<sub>25</sub>NaO<sub>92</sub><sup>+</sup>, [M + Na]<sup>+</sup> 3645.2811, found 3645.690.

#### 2.3. Synthesis of ketone-functionalized HexaHistidine

A 0.24 mmol/g of Rink-amide-ChemMatrix resin, Fmoc-His(trt)-OH (96  $\mu$ mol, 4.0 equivalents), and 5-oxohexanoic acid (4.0 equivalents) were used. Briefly, 0.24 mmol/g of Rink-amide-ChemMatrix resin was placed in a 5 ml Libra tube, washed sequentially with DMF and DCM followed by DCM swelling for 30 min. The swollen resin was washed with DMF. Fmoc-His(trt)-OH amino acid was pre-activated using 4 equivalents of HBTU, 4 equivalents of HOBT in DMF and 3 equivalents of DIEA for 30 sec. The pre-activated Fmoc-His(trt)-OH was then added to the resin and allowed to couple for 15 min at 50 °C under microwave irradiation. The resin was then washed subsequently with DMF, DCM and then DMF. To block the unreacted/uncoupled amino groups in the resin, acetyl capping was performed using DMF:Ac<sub>2</sub>O:DIEA (8.5:1.0:0.5) for 5 min at room temperature, washed with DMF, DCM and then DMF, then Fmoc deprotection using 20% piperidine in DMF followed by washing with DMF, DCM and then DMF and the cycle repeated for six (6) times. After Fmoc deprotection of the last Fmoc-His(trt)-OH, 5-oxohexanoic acid was pre-activated using 4 equivalents of HBTU, 4 equivalents of HOBT in DMF and 3 equivalents of DIEA for 30 sec. The pre-activated 5-oxohexanoic acid was then added to the peptide-resin mixture and allowed to couple for 15 min at 50 °C under microwave irradiation. The mixture was washed subsequently with DMF, DCM and then DMF. Deprotection and cleavage of the peptide from the resin was done by adding TFA:EDT:H<sub>2</sub>O (95:2.5:2.5) cocktail to the washed resin in ice for 30 min with shaking and then the shaking was continued at room temperature for additional 1 h. The deprotection and cleavage processes were monitored using MALDI-TOF/MS. The solution containing the synthesized peptide was drained. The resin was flushed subsequently with the same cocktail solution, acetic acid, and methanol. The filtrates were combined and concentrated by air drying, dissolved in 50% acetonitrile and lyophilized. The peptide was then purified using RP-HPLC with acetonitrile (B) and water (A) both with 0.1% TFA using Intersil® ODS-3 (5  $\mu$ m, 4.6 mm x 250 mm) column at room temperature, 1 ml/min flow rate, 220 nm wavelength for detection, and solvent gradient (A:B) of 90:10 (0 min), 70:30 (50 min), and 5:95 (60 min) to get the ketone-tagged HexaHis and then lyophilized [29–32].

MALDI-TOF/MS: *m/z* calcd for C<sub>42</sub>H<sub>54</sub>N<sub>19</sub>O<sub>8</sub><sup>+</sup>, [M + H]<sup>+</sup> 952.4405, found 952.880.

#### 2.4. Preparation of AO/PCSAM-QDs

To the 50  $\mu$ l of 1  $\mu$ M TOPO-QDs were added Isopropanol: Methanol (100  $\mu$ l: 50  $\mu$ l), then centrifuged at 15 000 g for 3 min. The solvent was removed and the pelleted TOPO-QDs were re-suspended in 50  $\mu$ l *n*-hexane and homogenized by sonication. TOPO-QDs/*n*-hexane solution was added with 30  $\mu$ l of Milli Q water, 1  $\mu$ l of NaBH<sub>4</sub> (12 wt % in 14 N NaOH), 5  $\mu$ l of 5 mM 11,11'-

dithio bis[undec-11-yl 12-(aminooxyacetyl)amino hexa(ethyleneglycol)] (HS-AO) and 10  $\mu$ l of 50 mM 11-mercaptopundecylphosphorylcholine (HS-PC). The mixture was mixed for 30 min at room temperature. The *n*-hexane layer containing TOPO were removed, and washed three times with hexane. The water layer containing AO/PCSAM-QDs was purified using ultra filtration (YM 10) and washed with ultrapure water (400  $\mu$ l) three times. The AO/PCSAM-QDs solution was directly analyzed by MALDI-TOFMS (Bruker Daltonics, Bremen, Germany) using DHB (1  $\mu$ l, 10 mg/ml) as a matrix [29].

### 2.5. Conjugation of QDs with ketone-functionalized peptides and glycopeptides

To the 10  $\mu$ l of AO/PCSAM-QDs solution was added 1  $\mu$ l of 10 mM ketone-functionalized peptides/glycopeptides and 1  $\mu$ l of 10 mM ketone-functionalized glycopeptide mixed thoroughly with 1  $\mu$ l of 10 mM HexaHis. The mixture was added with 10  $\mu$ l of 200 mM acetate buffer (pH 4.0), mixed for 15–30 min at room temperature and concentrated to dryness by centrifugal evaporator, to complete the oxime formation reaction, for 30 min at 40 °C. The obtained solid was resuspended in Milli Q, purified using ultra filtration (YM 10) and washed with Milli Q (400  $\mu$ l) three times. The products AO/PCSAM-QDs co-displaying the glycopeptide and HexaHis, AO/PCSAM-QDs carrying glycopeptides, AO/PCSAM-QDs carrying HexaHis were dissolved in Milli Q (10  $\mu$ l) to obtain 1  $\mu$ M solution. The samples were directly analyzed by MALDI-TOFMS using DHB (1  $\mu$ l, 10 mg/ml) as a matrix [29].

### 2.6. Cell culture

The A549 cells (Health Science Research Resource Bank) were grown in Dulbecco's Modified Eagle Medium (DMEM) and OUS-11 cells (Health Science Research Resource Bank) were grown in MEM at 37 °C with 5% CO<sub>2</sub>. All media used were supplemented with 10% (v/v) FBS, penicillin G (500 units/ml) and streptomycin (500 unit/ml) [33].

### 2.7. Cytotoxicity study

The A549 and OUS-11 cells were seeded in a 96-well plate (Thermo Scientific), at 5.0x10<sup>3</sup> cells/well, and incubated at 37°C with 5% CO<sub>2</sub> for 24 h. The cells were treated with HexaHis, compounds 1–4, AO/PCSAM-QD-1&HexaHis, AO/PCSAM-QD-2&HexaHis, AO/PCSAM-QD-3&HexaHis, and AO/PCSAM-QD-4&HexaHis for 24 h. Cell growth was determined by adding 10  $\mu$ l of cell counting kit 8 (Dojindo, Kumamoto, JAPAN), incubated for 2–4 h and optical density was measured using a model 550 Microplate reader (BioRad, Hercules, CA, USA) [33]. Data were reported in percent viability with respect to the untreated control ( $\pm$ SD) of the trials (*n* = 3).

### 2.8. Intracellular delivery of QD conjugates

Cellular internalization experiments were performed on an 8-well Nunc Lab-Tek II Chamber Slide System (Thermo Scientific™). Cells (5x10<sup>3</sup> cells/well) were seeded in the wells and cultured overnight. For the delivery experiments, QD-conjugates were diluted with the complete culture medium and incubated with cells at 37 °C with 5% CO<sub>2</sub> for 2 h. For assessing golgi

colocalization, the QD-conjugates were incubated with cells for 2 h. The excess QD-conjugates were removed by washing the cells with DPBS three times. The cells were then fixed with 4% paraformaldehyde for 10 min at room temperature and permeabilized with 0.4% Triton X-100 and washed. The cells were incubated with the golgi marker anti-giantin antibody [9B6] mouse IgG1 (abcam), as the primary antibody, for 1 h at room temperature or overnight at 4 °C, washed with DPBS three times and then incubated with secondary anti-body anti-IgG mouse Cy3 (Funakoshi, Japan) for 30 min to 1 h at room temperature. The nuclei were stained with Hoechst 33342 (Invitrogen), as the final hybridization process, and observed under fluorescence microscope [33].

### 2.9. Fluorescence microscopy and image analysis

The fluorescence microscope used for image acquisition and image analysis was an all-in-one fluorescence microscope BIOREVO BZ-9000 series generation II (Keyence, Japan) equipped with 4x, 20x, 40x, and 60x (oil immersion) lenses. Images were taken using standard filter set for DAPI (for Hoechst), FITC (for QD545) and TRITC (for anti-mouse IgG-Cy3). Merge images were generated and analyzed using BZ-II software [33].

### 2.10. Microarray

Boc-protected aminoxy coated slide was deprotected using 2M HCl for 2 h at 37 °C, washed 3x with ultrapure water and centrifuged at 2000 rpm for 2 min to dry. Different concentrations of heparin and ketone-functionalized peptides and glycopeptide, previously prepared using 50 mM AcOH reaction buffer, were machine plated onto the slide by BioChip-Arrayer machine (LASER TECHNO Co., Ltd.), incubated at 80 °C for 1 h, washed with miliQ water 3 times, and dried using centrifuge. The unreacted aminoxy groups were capped with succinic anhydride for 2 h at 37 °C, washed and dried. Heparin (Sigma-Aldrich) was added and allowed to interact at 37 °C for 2 h. Slide was washed with washing buffer, containing 0.05 wt% Triton X-100, 3 times followed by water. Mouse anti-heparin/heparin sulphate IgG antibody (Millipore) was added, incubated for 2 h at room temperature or at 4 °C overnight and washed subsequently with washing buffer and water 3 times. Secondary anti-body anti-IgG mouse Cy3 (Funakoshi, Japan) was added, allowed to react in the dark for 2 h at room temperature or at 4 °C overnight and washed with washing buffer 3 times. The slide was analyzed using GE Typhoon TRIO<sup>+</sup> variable mode imager (Amersham Biosciences).

## 3. Results and discussion

### 3.1. Peptides and glycopeptides syntheses and characterization

Both peptide and glycopeptide sequences used in this study were serglycin-like synthetic peptides and glycopeptides shown in Fig. 1 [18,23,30]. These were tetrapeptide composed of H-Ser<sup>1</sup>-Gly<sup>2</sup>-Ser<sup>3</sup>-Gly<sup>4</sup> (compound 1) and tetrapeptide with Gal $\beta$ (1–4)Xyl $\beta$ 1-(compound 2), where the sugar moieties were attached



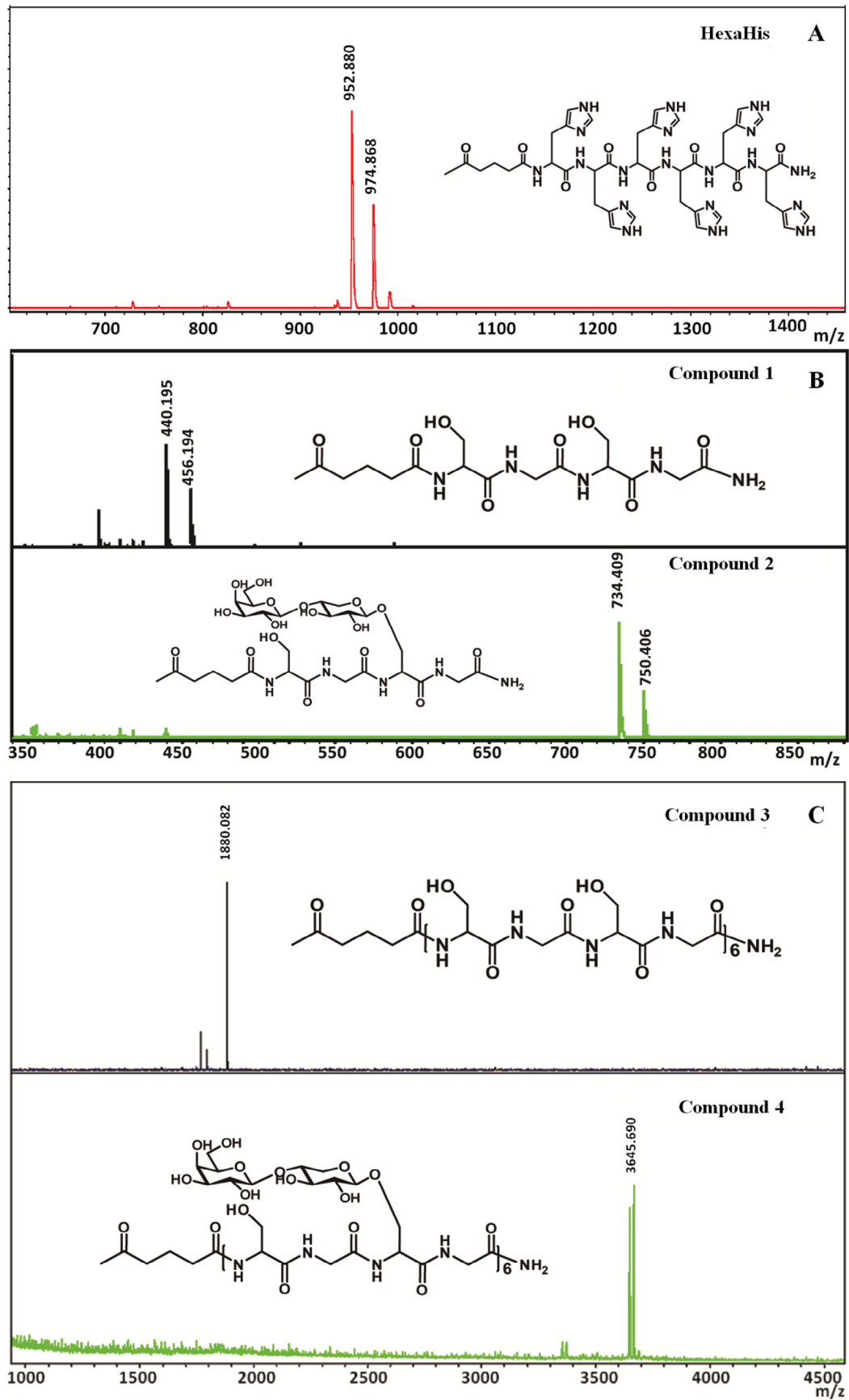


Fig. 2 – MALDI-TOF mass spectra of manually synthesized peptides and glycopeptides. (A) HexaHistidine, (B) monomer compounds 1 and 2, and (C) hexamer compounds 3 and 4.

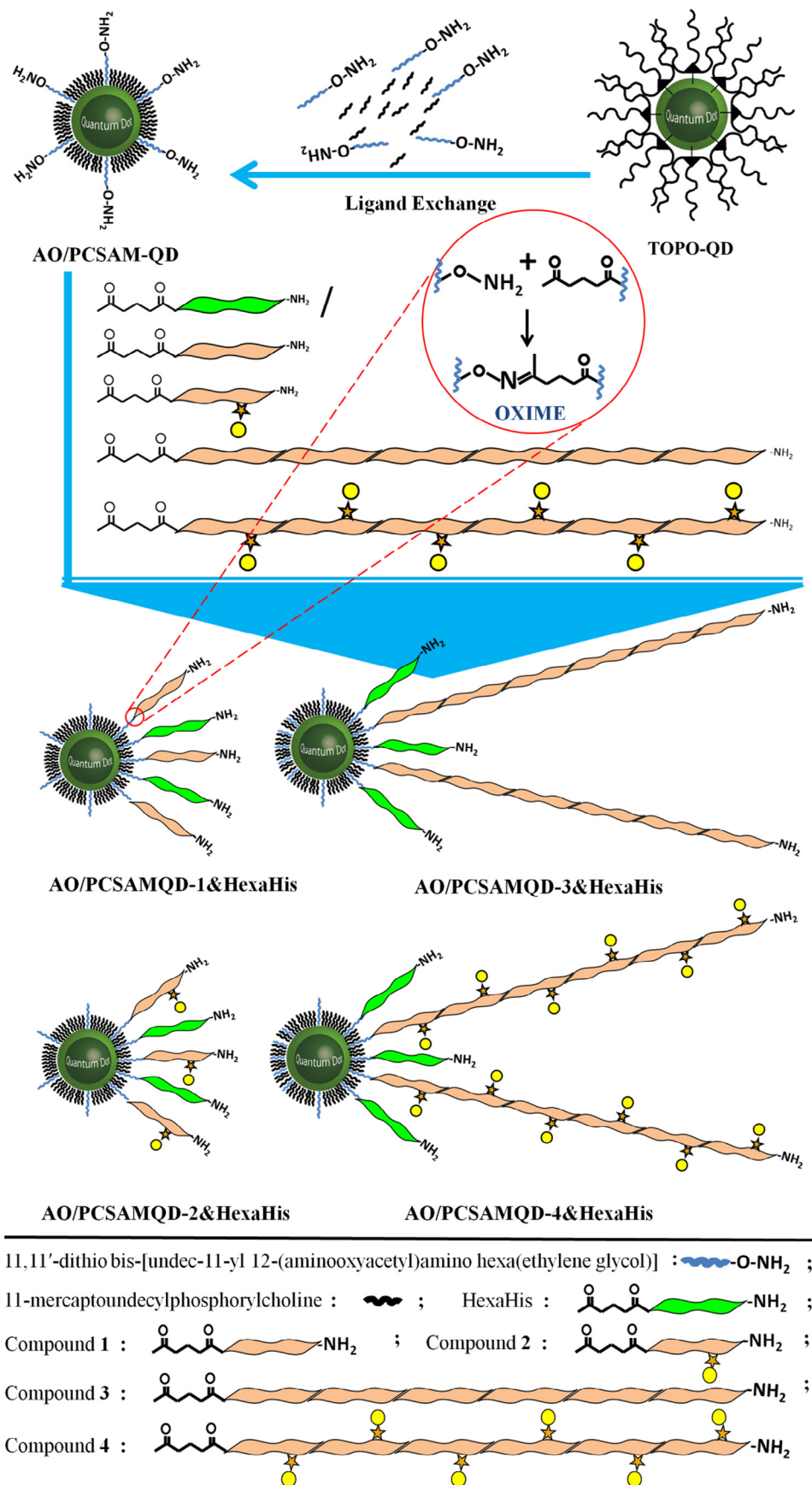
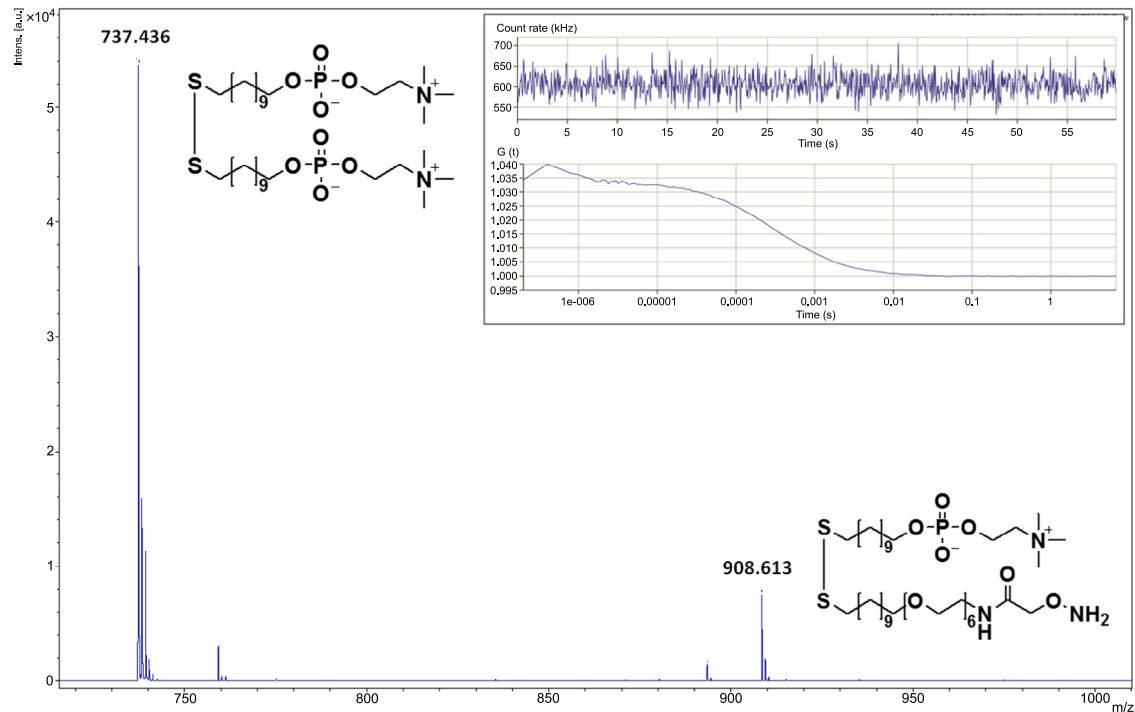


Fig. 3 – Standard protocol for the preparation of QD conjugates. Yellow circle represents galactose and orange star represents xylose.



**Fig. 4 – Characterization of AO/PCSAM-QDs (AO/PC = 1/20) carrying HexaHis and compounds 1-4 prepared by the standard protocol. Heterodimeric ions generated from QD conjugates during direct MALDI-TOFMS measured at positive mode and fluorescence fluctuation profile of AO/PCSAM-QDs measured by fluorescence correlation spectroscopy (inset).**

carrying HexaHis and 1 (AO/PCSAM-QD-1&HexaHis), AO/PCSAM-QDs carrying HexaHis and 2 (AO/PCSAM-QD-2&HexaHis), AO/PCSAM-QDs carrying HexaHis and 3 (AO/PCSAM-QD-3&HexaHis), and AO/PCSAM-QDs carrying HexaHis and 4 (AO/PCSAM-QD-4&HexaHis) as shown in Fig. 3. The formation of AO/PCSAM-QD-HexaHis, AO/PCSAM-QD-1&HexaHis, and AO/PCSAM-QD-2&HexaHis QD conjugates was confirmed by direct MALDI-TOF/MS shown in Fig. 5A, while for AO/PCSAM-QD-3&HexaHis and AO/PCSAM-QD-4&HexaHis in Fig. 5B. The

density of the displayed samples can affect the dispersion of the modified QDs in water and even in the serum-containing cell culture medium during cellular delivery. It was frequently observed that higher density of surface-displayed HexaHis with compounds 1-4 usually resulted to QD conjugate aggregation, which could certainly affect the internalization and dispersion of the QDs [33]. The good ratio between AOSH and PCSH was found to be 1:20, with good water dispersion and no observed significant aggregation [33].

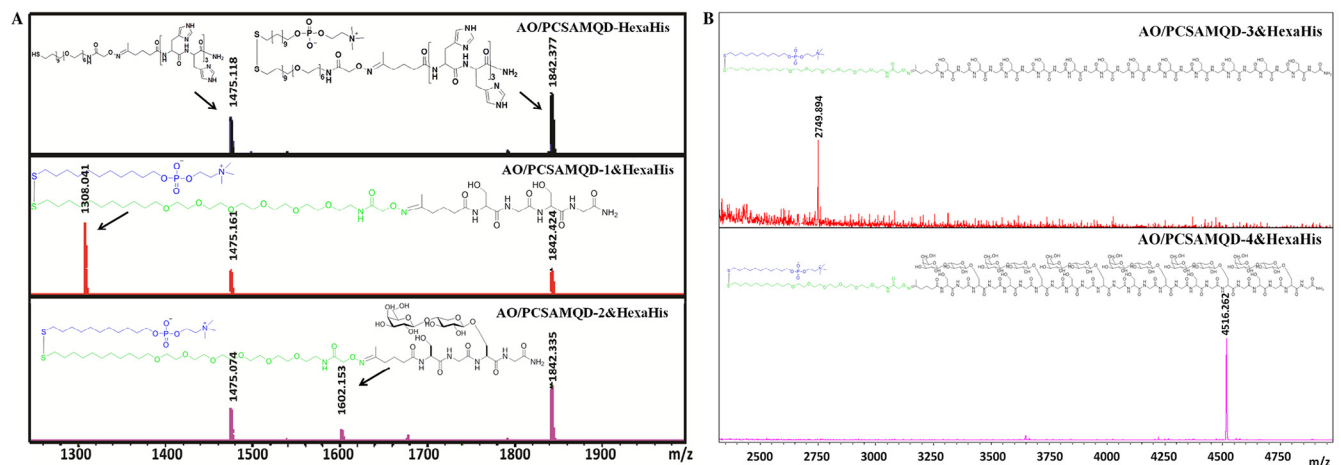


**Fig. 5 – Characterization of AO/PCSAM-QDs (AO/PC = 1/20) carrying HexaHis and compounds 1-4 using positive mode direct MALDI-TOFMS. (A) Heterodimeric ions generated from HexaHis-QD conjugates, HexaHis-QD conjugates containing compound 1, and compound 2. (B) Heterodimeric ions generated from HexaHis-QD conjugates containing compounds 3 and 4. Mass of HexaHis in B is not shown in the frame due to its very large mass difference.**

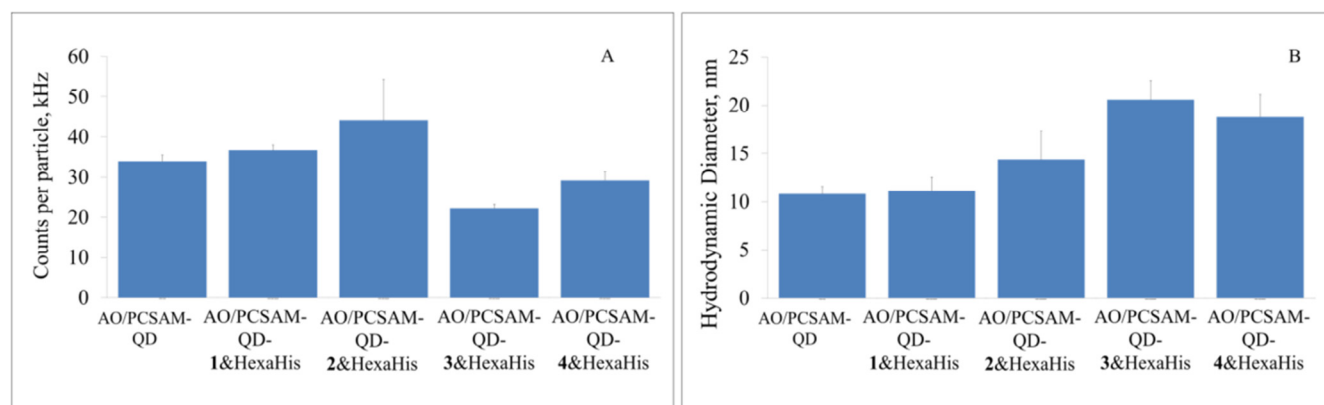


**Fig. 6 – Fluorescence Correlation Spectroscopy (FCS) data of the QD conjugates. (A) Fluorescence intensity per molecule and (B) the measured hydrodynamic diameter of AO/PCSAM-QDs (AO/PC = 1/20) carrying HexaHis and compounds 1–4 prepared by the standard protocol. Error bar represents SD.**

This strategy is so robust that any aldehyde- or ketone-functionalized molecule could be attached to AOSH via this type of conjugation, which in principle, could be used as general strategy for facile QD surface modification using an array of desired molecules to be displayed on QD surface. Individual fluorescence correlation spectrum also showed that prepared QD conjugates were highly dispersed in aqueous solution with no observed aggregation, making it highly viable candidate for intracellular delivery experiments, as shown in Fig. S1-S4. The fluorescent signals of the QD conjugates were also not significantly affected after the conjugation process as shown in their individual fluorescence fluctuation per molecule in Fig. 6A. This unaffected fluorescence signal per molecule is advantageous during QD conjugate detection and tracking inside the cell due to its sustained intensity of fluorescent signal that could be easily detected and classified from the background fluorescence.

#### 3.4. Cytotoxicity of peptides, glycopeptides, and QD conjugates

The problem with most of the nanoparticle-based delivering agents is their cytotoxicity. Aside from the core metal, molecules displayed on their surface could likely contribute to their cytotoxicity. To demonstrate that the cells are not adversely affected by QD conjugates, cytotoxicity assays were performed for all synthetic compounds and their QD conjugates. Results in Fig. 7 showed that all QD conjugates have no significant cytotoxicity towards the cell lines used. These ketone-functionalized peptides and glycopeptides were essentially noncytotoxic to the normal and lung cancer cell lines used.

#### 3.5. Intracellular Delivery of QD conjugates

The intracellular localization of QD conjugates were tracked during co-incubation with normal human lung tissue (OUS-11) and human lung adenocarcinoma (A549). For immunocytochemistry, golgi co-localization was assessed by tagging the golgi apparatus with golgi marker anti-giantin and detected using secondary antibody, while the nuclei were stained with Hoechst.

The co-conjugation with hexahistidine was primarily done to prevent endolysosomal sequestration of the QD conjugates, which could potentially degrade the peptides, glycopeptides, and glycans on the nanoparticle's surface through the action of hydrolytic enzymes such as proteases and glycosyl hydrolases [34], and could prevent their delivery to the exact intracellular compartment where they supposed to be delivered.

Co-incubation of the conjugates with OUS-11 and A549 revealed a different dynamics of QD conjugates inside the cancer and healthy human lung cell lines. In diseased cell line, A549 cells showed golgi uptake (pointed by white arrows) of all the QD conjugates carrying compounds 1–4 as shown in Fig. 8. However, a membrane-bound fluorescence (pointed by yellow arrows) of QD conjugates carrying compound 2 was evidently observed but not on its naked counterpart (QD conjugates carrying compound 1). The same phenomenon was also observed in QD conjugates carrying compound 4 and but not on its naked counterpart (QD conjugates carrying compound 3). It is likely that the observed membrane-bound fluorescence could be due to the interaction of the glycopeptides with its complementary lectins that are highly expressed on this cell line [35] and/or through QD conjugate interaction with heparin sulfate proteoglycans (HSPGs) on the cell surface, as shown in the microarray results in Fig. 9. The microarray result revealed that only the glycosylated peptides and HexaHis showed significant interaction with heparin, indicating that the intracellular entry of the QD conjugates is likely mediated by the interaction of HexaHis and glycopeptides with the glycosaminoglycans on the cell surface. It is also noteworthy that the QD conjugates carrying glycopeptides seem to have been directed specifically towards the golgi, while those QD conjugates carrying naked peptides were randomly distributed in the cytoplasm and the golgi (see Fig. 8, merge). These observations may suggest that, although A549 cells directed most of the QD conjugates to the golgi, the conjugates might have been delivered/trafficked inside the cell differently. Also, it seems likely that the QD conjugates carrying glycopeptides were not entering the cell all at once but rather in queues and that the remaining QD conjugates were interacting with the cell surface receptors and glycosaminoglycans waiting for their turn in endocytosis, as indicated by the population of QD conjugates that

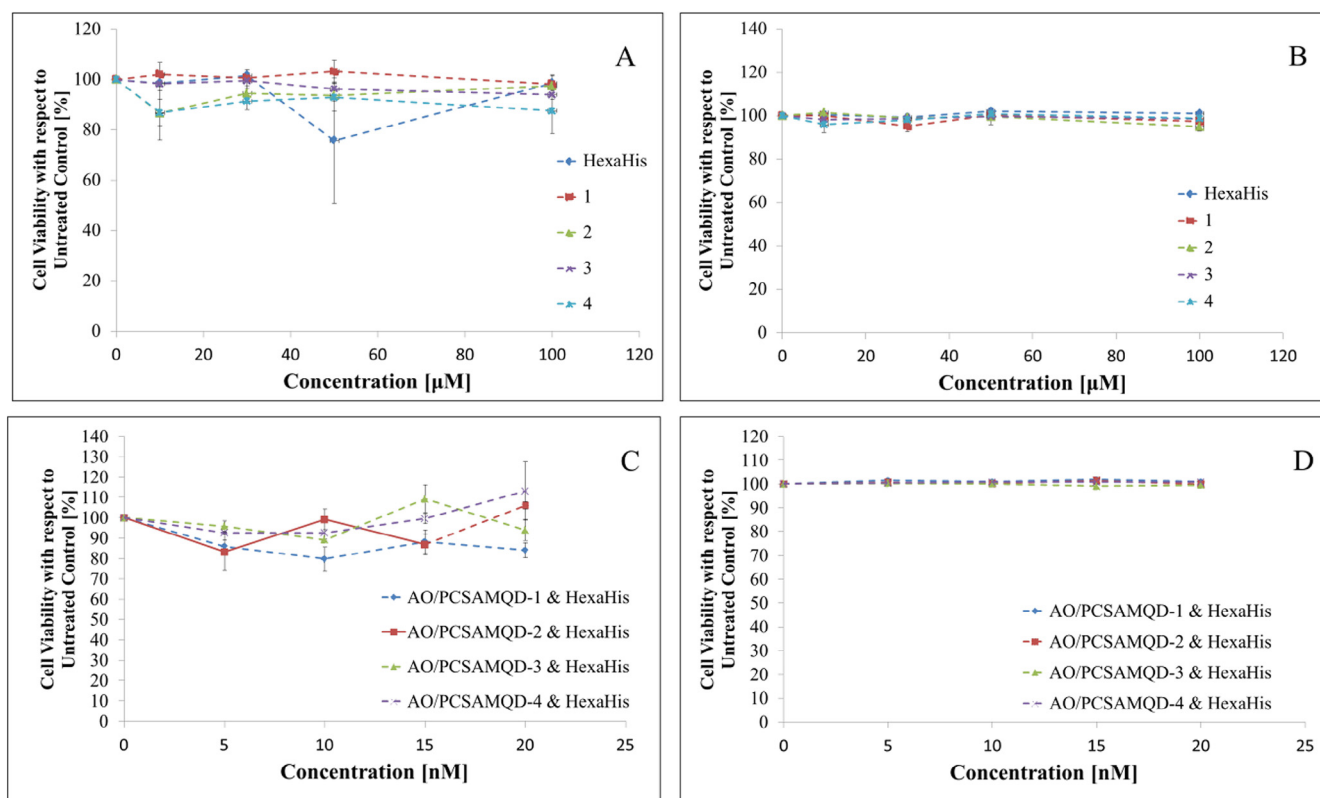


**Fig. 7 – Cytotoxicity Assay in OUS-11 and A549 cells. (A) Cytotoxicity of ketone-functionalized Peptides and Glycopeptides on OUS-11 and (B) cytotoxicity of ketone-functionalized Peptides and Glycopeptides on A549. (C) Cytotoxicity of AO/PCSAMQD carrying compounds 1–4 and HexaHis on OUS-11 and (D) Cytotoxicity of AO/PCSAMQD carrying compounds 1–4 and HexaHis on A549. Peptides and glycopeptides, as well as their corresponding QD conjugates AO/PCSAMQD carrying compounds 1–4 and HexaHis did not show adverse effect on cell viability of OUS-11 and A549. Error bar represents  $\pm$ SD.**

are actually inside the cell, and thus, their cellular delivery and localization mechanisms might have been strongly mediated by the presence of the glycan moiety.

In healthy cell line (OUS-11), the intracellular localization of QD conjugates greatly differed from the diseased cell line. The endocytosis of all QD conjugates in A549 was of higher rate [36], as indicated by the densely QD conjugate-populated cytoplasm, compared to the scarcely QD conjugate-populated cytoplasm of OUS-11 as shown in Fig. 10. Interestingly, OUS-11 cells showed no localization of QD conjugates displaying naked peptides (compounds 1 and 3) in the golgi, while those carrying glycopeptides 2 and 4 appeared to be distributed specifically in the golgi apparatus as shown by the yellow merged color resulted from the merged green and red colors from QD conjugates and golgi, respectively (Fig. 10, merge, pointed by white arrows). It appears that the presence of glycan moieties might have influenced the delivery of the conjugates, specifically to the golgi, and the absence of glycosylation may have restricted the conjugates from localizing in the golgi apparatus, which seems that the minimum requirement for golgi localization, in normal lung cells, was the presence of the sugar moiety in the polypeptide chain.

This study revealed an interesting finding that glycosylation could clearly govern sub-cellular localization of peptides on normal and lung cancer cells of the same type. It seems that

golgi localization, in normal cells, is only selective to the glycopeptides (Fig. 11). This difference in behavior between the normal and cancer cells in terms of trafficking QD conjugates could be linked to cancer cell's defective quality control and intracellular trafficking machineries.

#### 4. Conclusion

These observations warranted and exemplified the important role of glycosylation in intracellular compartmentalization. Although the complete mechanism remains unclear, normal human lung tissue cells can clearly discriminate glycosylated from non-glycosylated peptides, while human lung adenocarcinoma cannot distinguish the presence or absence of glycans on the peptide backbone. In this particular nanoparticle-based platform of delivery, the endocytosis of the QD conjugates were seemed to be mediated by the interaction of HexaHis and the glycopeptides with the glycosaminoglycans on the cell's surface.

This newly discovered difference in sub-cellular trafficking between normal and lung cancer cells could potentially be used as an effective strategy in targeted intracellular delivery by attaching glycosylated peptides to a carrier, containing

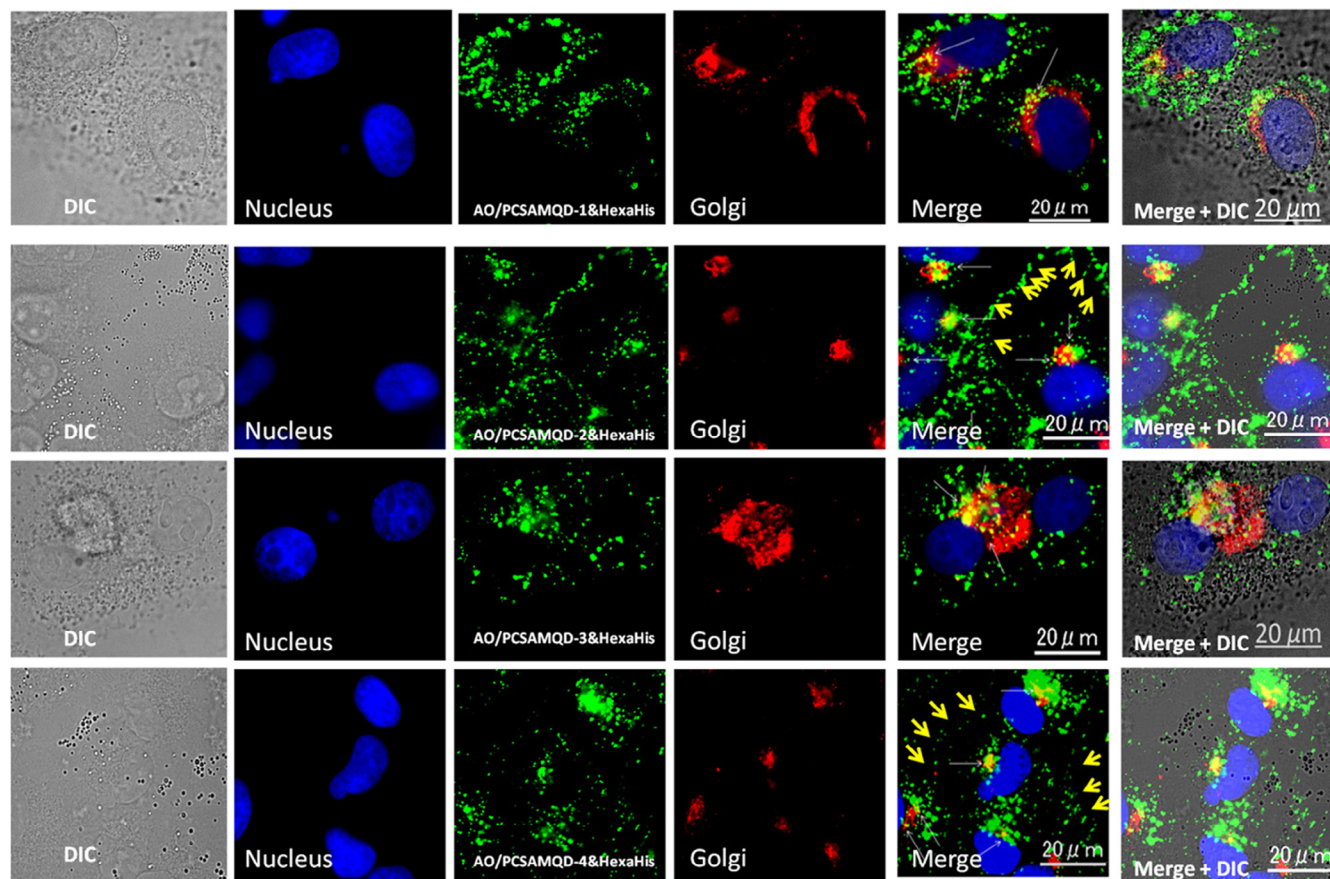


**Fig. 8 – Difference in Intracellular localization of QD conjugates containing compounds 1~4 in human lung adenocarcinoma (A549). Both glycosylated and non-glycosylated peptides, regardless of size, localized in the golgi. QD conjugates carrying glycopeptides (compounds 2 and 4) showed cell surface-bound fluorescent signal compared to QD conjugates carrying naked peptides (compounds 1 and 3). Cells were co-incubated with QD conjugates (green) for 2 h and fixed. Golgi apparatuses were stained with anti-giantin IgG and detected by secondary antibody (goat antimouse IgG H&L-Alexa Fluor647, red), while the nuclei were stained with Hoechst 33342 (blue). Merged yellow color indicates that the QD conjugates were localized in the golgi (pointed by thin white arrows). Yellow arrows point the cell surface-bound fluorescent signal of QD conjugates, indicating interaction between QD conjugates and the cell surface.**

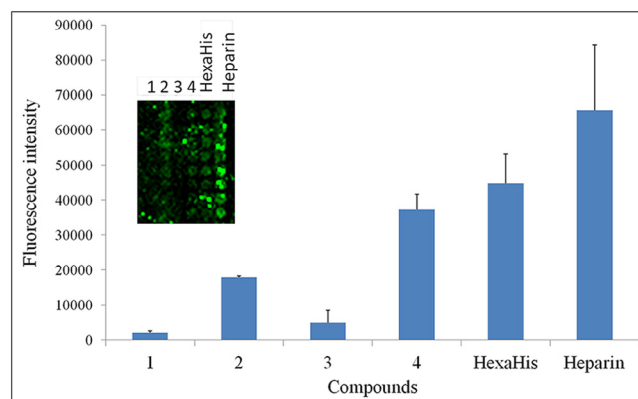


**Fig. 9 – Interaction of HexaHis and compounds 1~4 with glycosaminoglycan heparin using microarray. These interactions could prove the participation of GAGs in cellular membrane penetration of the QD conjugates as indicated by the interaction of the HixaHis and the glycosylated compounds 2 and 4 with heparin. Fluorescence Intensity is expressed in arbitrary unit (A.U) Error bars represent SD of  $n = 3$ .**

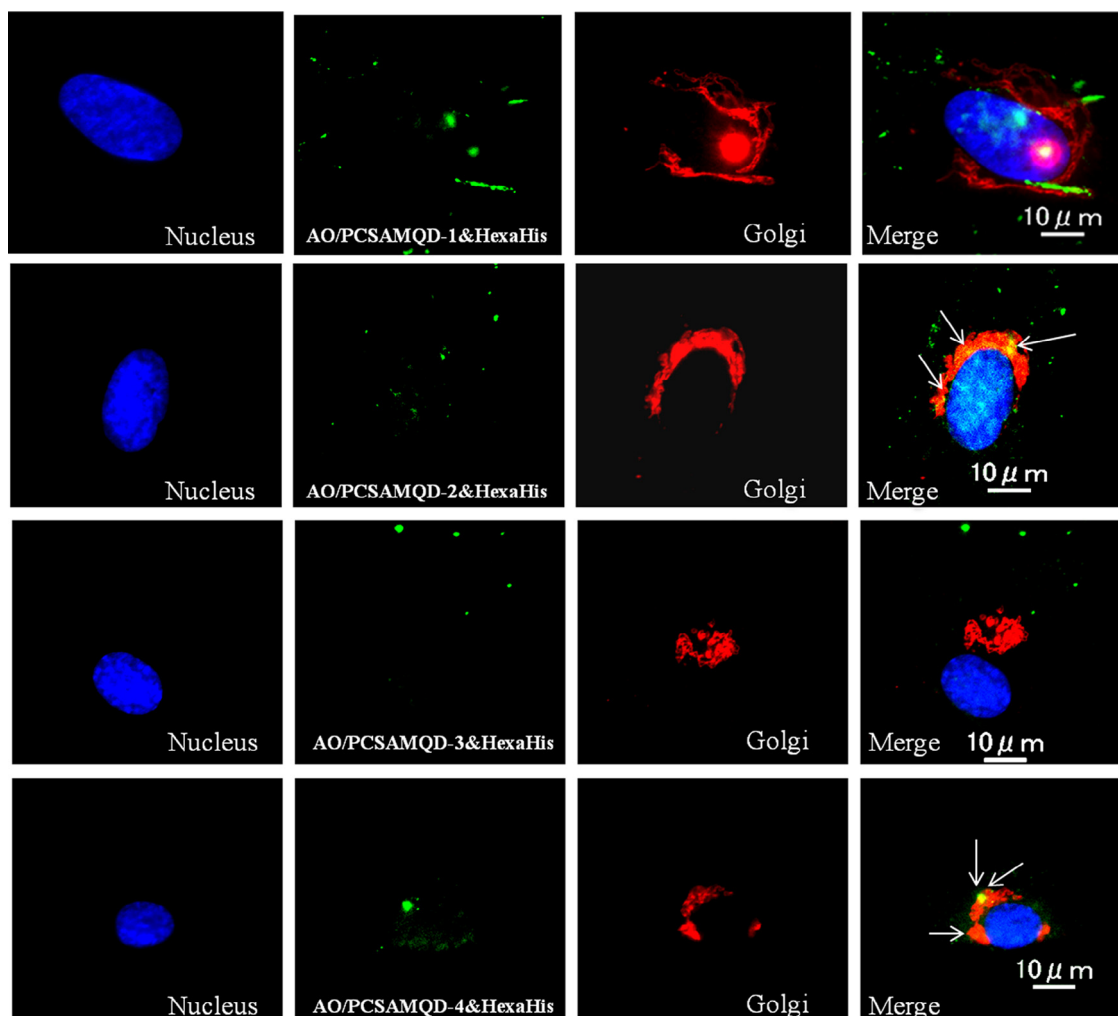


**Fig. 10 – Difference in Intracellular localization of QD conjugates containing compounds 1-4 in human normal lung tissue (OUS-11). Non-glycosylated peptides did not localize in the golgi of normal human lung tissue while glycosylated peptides localized in the golgi (pointed by white arrows). Cells were co-incubated with QD conjugates (green) for 2 h and fixed. Golgi apparatuses were stained with antigiantin IgG and detected by secondary antibody (goat antimouse IgG H&L-Alexa Fluor647, red), while the nuclei were stained with Hoechst 33342 (blue). Merged yellow color indicates that the QD conjugates were localized in the golgi (pointed by thin white arrows).**

therapeutic agents, to target golgi-resident enzymes for possible treatment of diseases associated with glycans and glycoproteins, such as, the congenital disease of glycosylation (CDG).

This very important detail in intracellular trafficking inside normal and cancer cells is an indispensable part in nanoparticle-based intracellular drug delivery.

### Conflict of Interest

The author reports no conflicts of interest. The author alone is responsible for the content and writing of this article.

### Acknowledgements

The author would like to thank Professor Doctor Shin-Ichiro Nishimura from the Faculty of Advanced Life Science, Hokkaido University, for the valuable assistance to complete the study, and the Ministry of Education, Culture, Science, and Technology, Japan.

### Appendix: Supplementary material

Supplementary data to this article can be found online at [doi:10.1016/j.ajps.2017.12.002](https://doi.org/10.1016/j.ajps.2017.12.002).

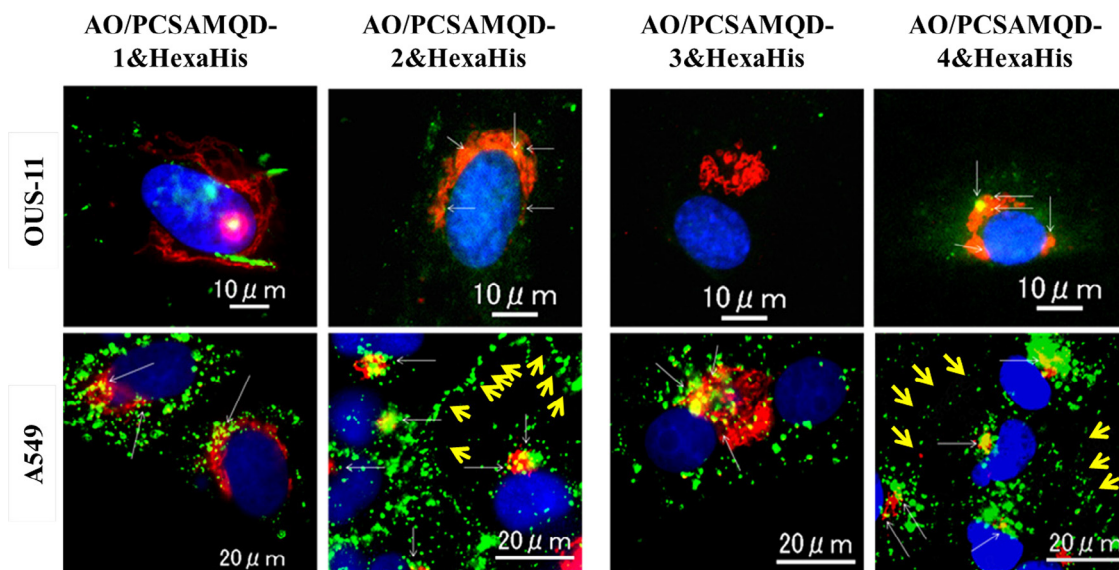


**Fig. 11 – Difference in Intracellular localization of compounds 1~4 in normal human lung tissue (OUS-11) and human lung adenocarcinoma (A549). Non-glycosylated peptides did not localized in the golgi of normal human lung tissue while glycosylated peptides localized in the golgi. In the case of human lung adenocarcinoma, all peptides, regardless of size and presence or absence of glycosylation, localized in the golgi. This observation showed significant influence of glycosylation on intracellular localization. Cells were co-incubated with QD conjugates (green) for 2 h and fixed. Golgi apparatuses were stained with antigiantin IgG and detected by secondary antibody (goat antimouse IgG H&L-Alexa Fluor647, red), while the nuclei were stained with Hoechst 33342 (blue). Merged yellow color indicates that the QD conjugates were localized in the golgi (pointed by white arrows). Yellow arrows point the cell surface-bound fluorescent signal of QD conjugates, indicating interaction between QD conjugates and the cell surface.**

## REFERENCES

- [1] Weerapana E, Imperiali B. Asparagine linked protein glycosylation: From eukaryotic to prokaryotic systems. *Glycobiology* 2006;16:91R-101R.
- [2] Mann M, Jensen ON. Proteomic analysis of post-translational modifications. *Nat Biotechnol* 2003;21:255-61.
- [3] Walsh CT, Garneau-Tsodikova S, Gatto GJ. Protein posttranslational modifications: The chemistry of proteome diversifications. *Angew Chem Int Ed Engl* 2005;44:7342-72.
- [4] Sears P, Wong CH. Enzyme action in glycoprotein synthesis. *Cell Mol Life Sci* 1998;54:223-52.
- [5] Lehle L, Strahl S, Tanner W. Protein glycosylation, conserved from yeast to man: A model organism helps elucidate congenital human diseases. *Angew Chem Int Ed Engl* 2006;45:6802-18.
- [6] Solá RJ, Rodríguez-Martínez JA, Griebenow K. Modulation of protein biophysical properties by chemical glycosylation: Biochemical insights and biomedical implications. *Cell Mol Life Sci* 2007;64:2133-52.
- [7] Freeze HH. Genetic defects in the human glycome. *Nature Reviews*. 2006;7:537-51.
- [8] Matsushita T, Ohyabu N, Fujitani N, et al. Site-specific conformational alteration induced by sialylation of MUC1 tandem repeating glycopeptide at an epitope region for anti-KL-6 monoclonal antibody. *Biochemistry* 2006;52:402-14.
- [9] Hashimoto R, Fujitani N, Takegawa Y, et al. An efficient approach for the characterization of mucin type glycopeptides: The effect of O-glycosylation on the conformation of synthetic mucin peptides. *Chem Eur J* 2011;17:2393-404.
- [10] Shimizu HK, Hosoguchi K, Liu Y, et al. Chemical synthesis, folding and structural insights into O-fucosylated epidermal growth factor-like repeat 12 of mouse Notch-1 receptor. *J Am Chem Soc* 2010;132:14857-65.
- [11] Shental-Bechor D, Levy Y. Effect of glycosylation on protein folding: A close look at thermodynamic stabilization. *PNAS* 2008;105:8256-61.
- [12] Öberg F, Sjöhamn J, Fischer G, Moberg A, Pedersen A, Neutze R, et al. Glycosylation Increases the Thermostability of Human Aquaporin 10 Protein. *J Biol Chem* 2011;286:31915-23.
- [13] Sinclair AM, Elliott S. Glycoengineering: The effect of glycosylation on the properties of therapeutic proteins. *J Pharm Sci* 2005;94:1626-35.
- [14] Liu DT. Glycoprotein pharmaceuticals: Scientific and regulatory considerations, and the US Orphan Drug Act. *Trends Biotechnol* 1992;10:114-20.
- [15] Dennis JW, Lau KS, Demetriou M, et al. Adaptive regulation at the cell surface by N-glycosylation. *Traffic* 2009;10:1569-78.
- [16] Hoseki J, Ushioda R, Nagata K. Mechanism and components of endoplasmic reticulum-associated degradation. *J Biochem* 2010;147:19-25.
- [17] Kollmann K, Pohl S, Marschner K, et al. Mannose phosphorylation in health and disease. *Eur J Cell Biol* 2010;89:117-23.
- [18] Watson P, Jones AT, Stephens DJ. Intracellular trafficking pathways and drug delivery: fluorescence imaging of living and fixed cells. *Adv Drug Delivery Rev*. 2005;57:43-61.
- [19] Lloyd JB. Lysosome membrane permeability: implications for drug delivery. *Adv Drug Deliv Rev* 2000;41:189-200.

- [20] Wattiaux R, Laurent N, Wattiaux-De Coninck S, et al. Endosomes, lysosomes: their implication in gene transfer. *Adv Drug Deliv Rev* 2000;41:201-8.
- [21] Jones AT, Gumbleton M, Duncan R. Understanding endocytic pathways and intracellular trafficking: a prerequisite for effective design of advanced drug delivery systems. *Adv Drug Deliv Rev* 2003;55:1353-7.
- [22] Conner SD, Schmid SL. Regulated portals of entry into the cell. *Nature* 2003;422:37-44.
- [23] Bonifacino JS, Glick BS. The mechanisms of vesicle budding and fusion. *Cell* 2004;116:153-66.
- [24] Maxfield FR, McGraw TE. Endocytic recycling. *Nat Rev Mol Cell Biol* 2004;5:121-32.
- [25] Hoshi H, Shimawaki K, Takegawa Y, et al. Molecular shuttle between extracellular and cytoplasmic space allows for monitoring of GAG biosynthesis in human articular chondrocytes. *Biochim Biophys Acta* 2012;1820:1391-8.
- [26] Cai W, Shin DW, Chen K, et al. Peptide-labeled near-infrared quantum dots for imaging tumor vasculature in living subjects. *Nano Lett* 2006;6:669-76.
- [27] De la Fuente JM, Penades S. Glyco-quantum dots: a new luminescent system with multivalent carbohydrate display. *Tetrahedron Asymm*. 2005;16:387-91.
- [28] Robinson A, Fang JM, Chou PT, et al. Probing Lectin and Sperm with Carbohydrate-Modified Quantum Dots. *J. Chembiochem* 2005;6:1899-905.
- [29] Ohyanagi T, Nagahori N, Shimawaki K, et al. Importance of Sialic Acid Residues Illuminated by Live Animal Imaging Using Phosphorylcholine Self-Assembled Monolayer-Coated Quantum Dots. *J Am Chem Soc* 2011;133:12507-17.
- [30] Shimawaki K, Fujisawa Y, Sato F, et al. Highly Efficient and Versatile Synthesis of Proteoglycan Core Structures from 1,6-Anhydro-b-lactose as a Key Starting Material. *Angew Chem Int Ed Engl* 2007;46:3074-9.
- [31] Matsushita T, Hinou H, Kurogochi M, et al. Rapid microwave assisted solid-phase glycopeptide synthesis. *Org Lett* 2005;7:877-80.
- [32] Garcia-Martin F, Hinou H, Matsushita T, et al. An efficient protocol for the solid-phase synthesis of glycopeptides under microwave irradiation. *Org Biomol Chem* 2012;10:1612-7.
- [33] Tan RS, Naruchi K, Amano M, et al. Rapid Endolysosomal Escape and Controlled Intracellular Trafficking of Cell Surface Mimetic Quantum-Dots-Anchored Peptides and Glycopeptides. *ACS Chem Biol* 2015;10:2073-86.
- [34] Tan RS, Hinou H, Nishimura S-I. Novel  $\beta$ -galactosynthase -  $\beta$ -mannosynthase dual activity of  $\beta$ -galactosidase from *Aspergillus oryzae* uncovered using monomer sugar substrates. *RSC Adv* 2016;6:50833-6.
- [35] Kuo P-L, Huang M-S, Cheng D-E, et al. Lung Cancer-derived Galectin-1 Enhances Tumorigenic Potentiation of Tumor-associated Dendritic Cells by Expressing Heparin-binding EGF-like Growth Factor. *J Biol Chem* 2012;287:9753-64.
- [36] Fuster MM, Esko JD. The sweet and sour of cancer: glycans as novel therapeutic targets. *Nat Rev Cancer* 2005;5:526-42.